Asymptotic analysis of silicon based Bragg fibers

Yong Xu, and Amnon Yariv

Department of Applied Physics, MS 128-95, California Institute of Technology, Pasadena, CA 91125

yong@its.caltech.edu

James G. Fleming, and Shawn-Yu Lin

MEMS and Novel Silicon Technologies, Sandia National Laboratories, Albuquerque, NM 87185-1080

Abstract: We developed an asymptotic formalism that fully characterizes the propagation and loss properties of a Bragg fiber with finite cladding layers. The formalism is subsequently applied to miniature air-core Bragg fibers with Silicon-based cladding mirrors. The fiber performance is analyzed as a function of the Bragg cladding geometries, the core radius and the material absorption. The problems of fiber core deformation and other defects in Bragg fibers are also addressed using a finite-difference time-domain analysis and a Gaussian beam approximation, respectively.

OCIS codes: (130.2790) Guided waves; (230.7370) Optical design and fabrication

References and links

1. P. Yeh, A. Yariv, and E. Marom, "Theory of Bragg fiber," J. Opt. Soc. Am. **68**, 1196-1201 (1978).
2. Y. Fink, D. J. Ripin, S. Fan, C. Chen, J. D. Joannopoulos, and E. L. Thomas, "Guiding optical light in air using an all-dielectric structure," J. Lightwave Technol. **17**, 2039-2041 (1999).
3. S. G. Johnson et al., "Low loss asymptotically single-mode propagation in large-core Omniguide fibers," Opt. Express **9**, 748-779 (2001). http://www.opticsexpress.org/abstract.cfm?URI=OPEX-9-13-748.
4. Y. Xu, R. K. Lee, and A. Yariv, "Asymptotic analysis of Bragg fibers," Opt. Lett. **25**, 1756-1758 (2000).
5. Y. Xu, G. X. Ouyang, R. K. Lee, and A. Yariv, "Asymptotic matrix theory of Bragg fibers," J. Lightwave Technol. **20**, 428-440 (2002).
6. J. Marcou, F. Brechet, and P. Roy, "Design of weakly guiding Bragg fibres for chromatic dispersion shifting towards short wavelengths," J. Opt. A, **3**, S144-S153 (2001).
7. A. Argyros, "Guided modes and loss in Bragg fibres," Opt. Express, **10**, 1411-1417, (2002). http://www.opticsexpress.org/abstract.cfm?URI=OPEX-10-24-1411.
8. J. G. Fleming, S. Y. Lin, and R. Hadley, in Proceeding of the solid-state sensor actuator and microsystems workshop, p.p. 173, (Hilton Head, S.C., 2002).
9. R. F. Cregan, B. J. Mangan, J. C. Knight, T. A. Birks, P. St J. Russell, P. J. Roberts, and D. C. Allan, "Single-mode photonic band gap guidance of light in air," Science **285**, 1537-1539 (1999).
10. A. Taflove, S. C. Hagness, *Computational electrodynamics: the finite-difference time-domain method*, (Artech house, Boston, 2000).
11. See for example, A. Yariv, *Optical electronics in modern communications*, Chapter 2, (Oxford university press, New York, 1997).

1. Introduction

Bragg fibers, which are composed of a low index core (possibly air) surrounded by alternating annular layers with different dielectric constants, were first proposed by Yeh *et al.* [1] in 1978. A schematic of a Bragg fiber is shown in Fig. 1. The possibility of guiding light in air by Bragg fibers [2, 3, 4, 5, 6, 7, 8] or photonic crystal fibers [9] has recently attracted a lot of attention. Omni-fibers [2, 3], which are Bragg fibers with very large cladding indices contrast, have

#2230 - $15.00 US Received March 14, 2003; Revised April 25, 2003

been experimentally demonstrated. Miniature Bragg fibers with silicon based cladding materials such as Si and Si_3N_4, were recently fabricated by J. Fleming *et al.* [8] using combinations of etching and CVD (chemical vapor deposition). The silicon based miniature Bragg fibers are developed for integrated optics applications such as thermo-optical switches and BioMEMS devices, which require properties quite different from other types of Bragg fibers intended for telecommunication applications. For example, Bragg fibers for integrated optics applications can tolerate propagation loss of the order of dB/cm, rather than <dB/km demanded by telecommunication fibers.

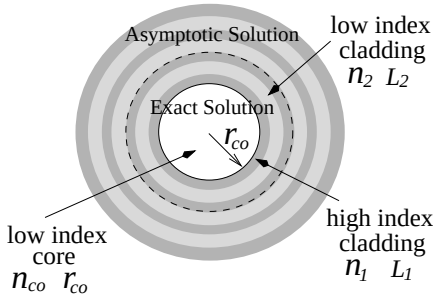

Fig. 1. Schematics of a Bragg fiber. In this paper, we assume the low index core is air ($n_{co} = 1$) and has radius of r_{co}. The refractive index and the thickness of the cladding layers are respectively n_1, L_1, and n_2, L_2. The dashed line represents the interface between the "exact solution" region and the "asymptotic solution" region.

As in the case of step-index optical fibers, two of the most important parameters of Bragg fibers are the modal dispersion and the propagation loss. In Ref. [4] and Ref. [5], we have developed an asymptotic formalism that greatly simplifies the analysis of a Bragg fiber. Here we incorporate a leaky mode method [3, 7] into this asymptotic formalism. The extended asymptotic approach developed in this paper is capable of fully characterizing the dispersion and loss of the Bragg fiber, while retaining the simplicity and physical transparency of the original asymptotic approach. Next, we apply the asymptotic approach to analyze the guiding behavior of a miniature Bragg fiber as reported in Ref. [8] as a function of the absorption in the cladding layers, the geometries of the Bragg cladding, and the core radius. We find that only four pairs of Si/Si_3N_4 cladding pairs are required to achieve propagation loss below 1dB/cm. From the asymptotic analysis results, we establish that the material absorption in the Si cladding layers has little influence on the propagation loss of the guided air-core modes. We obtain a simple formula that characterizes the exponential reduction of the modal propagation loss as the number of cladding pairs increases. We find that the quarter-wave stack cladding geometry, which is commonly used in the literature, does not necessarily lead to optimal guiding.

Due to the fabrication processes, it is difficult to realize the miniature Bragg fibers with perfect cylindrical symmetry. Using the finite difference time domain (FDTD) simulations, we investigate a deformed Bragg fiber and demonstrate that the Bragg fiber dispersion is insensitive to the air core deformation. However, the guided modes in the deformed fiber are no longer cylindrically symmetric, which may lead to a higher propagation loss. Due to the CVD processes, the Bragg fibers also have gas inlet ports along the fibers at intervals about hundreds of microns. Drawing analogy with free space diffraction of a Gaussian beam, we estimate the excessive loss associated with the presence of the gas inlet ports.

2. Asymptotic analysis

The approach outlined in this section is an extension of the asymptotic formalism developed in Ref. [4] and Ref. [5]. The key difference is that here we allow the propagation constant β to be complex, with $\beta = \beta_r + i\beta_i$ (see also Ref. [3] and Ref. [7]). The real part β_r determines

#2230 - $15.00 US Received March 14, 2003; Revised April 25, 2003

the dispersion properties of the Bragg fiber modes, and the imaginary part β_i gives the modal loss. We also allow the dielectric constants of the cladding media to be complex to account for the material absorption. The main advantages of the asymptotic formalism are its simplicity and physical transparency, especially when we need consider both TE and non-TE polarized modes. More specifically, in the asymptotic analysis, we approximate electromagnetic fields in the Bragg fiber cladding layers as $\exp(\pm ikr)/\sqrt{r}$, which behave similarly to those in a planar Bragg stack. In Ref. [4], this similarity allows us to derive an analytical expression for the dispersion of the Bragg fiber modes.

It can be shown that the guided Bragg fiber mode can be determined from the four electromagnetic field components E_z, H_θ, H_z, and E_θ [1]. From symmetry consideration alone, we can label each guided mode according to its angular frequency ω, propagations constant β, and the "azimuthal quantum number" m, with the functional dependence of $\exp(i\omega t - i\beta z)\exp(im\theta)$. In the nth dielectric layer, the radial dependence of the guided mode can be written as [1]:

$$\begin{bmatrix} E_z \\ H_\theta \\ H_z \\ E_\theta \end{bmatrix} = M_n(r) \begin{bmatrix} A_n \\ B_n \\ C_n \\ D_n \end{bmatrix}, \tag{1}$$

where $M_n(r)$ is a 4×4 matrix, and the field amplitude constants A_n, B_n, C_n, and D_n are constant within the nth dielectric layer.

In the asymptotic formalism, we separate the dielectric layers of the Bragg fiber into two groups, where the exact solutions are used for the layers of the inner region, while the asymptotic approximation of the exact solutions is used for the outer region. (see Fig. 1). In the "exact solution" region, the 4×4 matrix $M_n(r)$ is defined as [1]:

$$M_n(r) = \begin{bmatrix} J_m(k_n r) & Y_m(k_n r) & 0 & 0 \\ \frac{-i\omega\varepsilon_0\varepsilon_n}{k_n} J'_m(k_n r) & \frac{-i\omega\varepsilon_0\varepsilon_n}{k_n} Y'_m(k_n r) & \frac{m\beta}{k_n^2 r} J_m(k_n r) & \frac{m\beta}{k_n^2 r} Y_m(k_n r) \\ 0 & 0 & J_m(k_n r) & Y_m(k_n r) \\ \frac{m\beta}{k_n^2 r} J_m(k_n r) & \frac{m\beta}{k_n^2 r} Y_m(k_n r) & \frac{i\omega\mu_0}{k_n} J'_m(k_n r) & \frac{i\omega\mu_0}{k_n} Y'_m(k_n r) \end{bmatrix}, \tag{2}$$

where ε_n is the dielectric constant of the nth layer, and k_n is

$$k_n = \sqrt{\varepsilon_n \omega^2/c^2 - \beta^2}\,. \tag{3}$$

It should be emphasized that ε_n can be a complex number, with its imaginary part accounting for the material absorption in the nth dielectric layer. If the nth dielectric layer belongs to the "asymptotic solution" region, the 4×4 matrix $M_n(r)$ take the form of [4, 5]:

$$M_n(r) = \frac{1}{\sqrt{r}} \begin{bmatrix} e^{-ik_n r} & e^{ik_n r} & 0 & 0 \\ -\frac{\omega\varepsilon_0\varepsilon_n}{k_n} e^{-ik_n r} & \frac{\omega\varepsilon_0\varepsilon_n}{k_n} e^{ik_n r} & 0 & 0 \\ 0 & 0 & e^{-ik_n r} & e^{ik_n r} \\ 0 & 0 & \frac{\omega\mu_0}{k_n} e^{-ik_n r} & -\frac{\omega\mu_0}{k_n} e^{ik_n r} \end{bmatrix}. \tag{4}$$

We notice that Eq. (4) is block-diagonal. As a result, the TM modes with field components E_z and H_θ, are decoupled from the TE modes which consist of H_z and E_θ.

The four field amplitude constants (A_{n+1}, B_{n+1}, C_{n+1}, and D_{n+1}) in the $(n+1)$th layer can be derived from the corresponding quantities in the adjacent nth layer by requiring the continuity of E_z, H_θ, H_z, and H_θ across the interface between the two dielectric layers [5]:

$$\begin{bmatrix} A_{n+1} \\ B_{n+1} \\ C_{n+1} \\ D_{n+1} \end{bmatrix} = [M_{n+1}(\rho_n)]^{-1} M_n(\rho_n) \begin{bmatrix} A_n \\ B_n \\ C_n \\ D_n \end{bmatrix}, \tag{5}$$

#2230 - $15.00 US Received March 14, 2003; Revised April 25, 2003

where ρ_n is the radius of the interface between the nth dielectric layer and the $(n+1)$th dielectric layer, M_n and M_{n+1} are defined according to Eq. (2) or Eq. (4), depending on whether the dielectric layer belongs to the inner "exact solution" region or to the outer "asymptotic solution" region. We can apply Eq. (5) iteratively and relate the field amplitude constants outside of the Bragg fiber (A_{out}, B_{out}, C_{out}, and D_{out}) to the corresponding quantities within the low index core (A_{core}, B_{core}, C_{core}, and D_{core}) via a 4×4 transfer matrix:

$$\begin{bmatrix} A_{out} \\ B_{out} \\ C_{out} \\ D_{out} \end{bmatrix} = \begin{bmatrix} t_{11} & t_{12} & t_{13} & t_{14} \\ t_{21} & t_{22} & t_{23} & t_{24} \\ t_{31} & t_{32} & t_{33} & t_{34} \\ t_{41} & t_{42} & t_{43} & t_{44} \end{bmatrix} \begin{bmatrix} A_{core} \\ B_{core} \\ C_{core} \\ D_{core} \end{bmatrix} . \tag{6}$$

We require that the electromagnetic field must be finite within the low index core and that the electromagnetic field outside of the fiber consists of only the outgoing radiation field. Such boundary conditions lead to $B_{core} = D_{core} = 0$ and $B_{out} = D_{out} = 0$, respectively. Substituting these two requirements into Eq. (6), we obtain:

$$\mathbf{T}\begin{bmatrix} A_{core} \\ C_{core} \end{bmatrix} = 0 , \ \mathbf{T} = \begin{bmatrix} t_{21} & t_{23} \\ t_{41} & t_{43} \end{bmatrix} . \tag{7}$$

The complex propagation constant β of any guided mode is given by the condition of $\det(\mathbf{T}) = 0$, and the field distribution can be obtained from the eigenvector $[A_{core} \ \ B_{core}]$ that corresponds to the zero eigenvalue of the 2×2 matrix $\mathbf{T}$.

3. Guiding in silicon-based miniature Bragg fibers

3.1 Dispersion and loss in a specific Bragg fiber geometry

We first apply the asymptotic formalism to analyze the dispersion and propagation loss of the guided modes in a Bragg fiber as reported by J. Fleming *et al.* in Ref. [8]. The fiber consists of four pairs of Si/Si_3N_4 mirror stacks, with Si being the innermost cladding layer. For the polysilicon layers, we use a refractive index $n_1 = 3.5$ and thickness $L_1 = 0.11\mu m$. The refractive index of the Si_3N_4 layer is $n_2 = 2.0$ and its thickness is $L_2 = 0.21\mu m$. The air core radius is $r_{co} = 7.5\mu m$. The bulk absorption in the polysilicon layer is estimated to be about 10dB/cm. In our analysis, we assume that the "exact solution" region consists of the five innermost dielectric layers, whereas the rest of the structure is described by the asymptotic solutions. With a large air core radius, the Bragg fiber supports multiple guided modes, which are labeled according to their "azimuthal quantum number" m followed by the number of zeros of the electromagnetic field in the air core. We limit ourselves to the first two TE modes (TE01 and TE02), the fundamental TM mode (TM01), and the fundamental mixed polarization mode (HE11).

In Fig. 2(a), we plot the E_θ field of the TE01 mode at the wavelength of $1.65\mu m$. We notice that the E_θ component is zero at the interface between the air core and the Si layer, which has been explained by drawing an analogy to perfect metal [3, 7]. From a more fundamental point of view, the condition of $E_\theta = 0$ at the air/Si interface leads to maximum reduction of the E_θ field amplitude within the Si cladding layer [1], which in turn results in minimum propagation loss. Combining the condition of $E_\theta = 0$ at $r = r_{co}$ with the fact that TE modes take the form of $J_1(\sqrt{\omega^2/c^2 - \beta^2}r)$ within the air core, we find

$$n_{eff}^{TE0i} = \sqrt{1 - (\frac{x_{1i}\lambda}{2\pi r_{co}})^2} , \tag{8}$$

where x_{1i} is the ith zero of the first order Bessel functions, i.e. $J_1(x_{1i}) = 0$. This relation has been given in Ref. [7]. Using the asymptotic approach, we calculate the effective indices (defined as

#2230 - $15.00 US Received March 14, 2003; Revised April 25, 2003

$\beta_r c/\omega$) of the TE01, TE02, TM01, and HE11 modes and plot the results in Fig. 2(b). The effective indices of the TE01 and TE02 modes, predicted by Eq. (8), are also shown in Fig. 2(b) as solid lines. It is clear that Eq. (8) is in excellent agreement with the calculated dispersion of the TE modes.

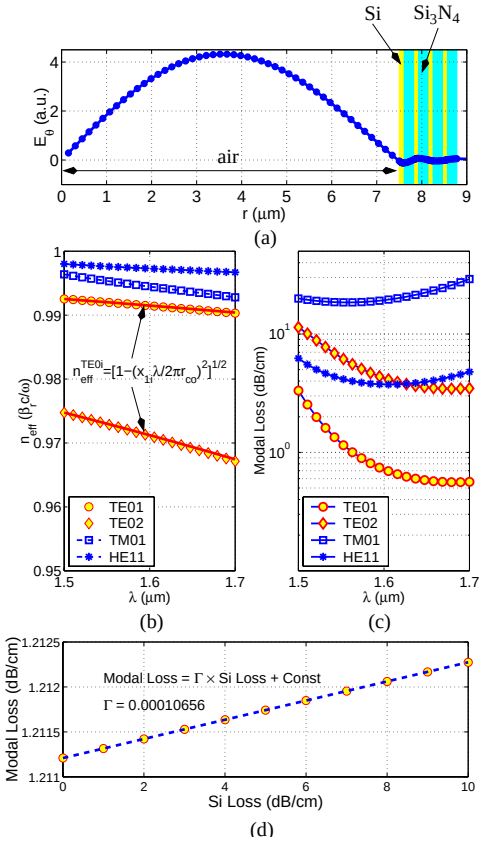

Fig. 2. The asymptotic results of an air-core Bragg fiber with $r_{co} = 7.5\mu m$, $n_1 = 3.5$ and $L_1 = 0.11\mu m$, $n_2 = 2.0$ and $L_2 = 0.21\mu m$. (a) The E_θ component of the TE01 mode at $\lambda = 1.65\mu m$. (b) The effective indices of the TE01, TE02, TM01, and HE11 modes. (c) The loss of the TE01, TE02, TM01, and HE11 modes. In (a), (b) and (c), we set the absorption loss in the Si layer to be 10dB/cm. (d) The loss of the TE01 mode at $\lambda = 1.55\mu m$ with Si layer loss varying from 0dB/cm to 10dB/cm. The dashed line is a linear fit of the asymptotic results.

The loss of the TE01, TE02, TM01, and HE11 modes are shown in Fig. 2(c) within the wavelength range of 1500nm to 1700nm. As expected, the TE01 mode has the lowest loss, between 0.5 to 2 dB/cm within the wavelength range of interest. It should be mentioned that the experimentally realized miniature Bragg fiber deviates considerably from the circular shape, which may lead to higher loss and will be discussed in the next section. Another feature of Fig. 2(c) is that the TE02 mode and the HE11 mode have similar loss, about 5 times higher than that of the fundamental TE01 mode, whereas in other realizations of Bragg fibers [3], non-TE polarized modes generally have loss far greater than that of the higher order TE modes. Experimentally, guiding in miniature Bragg fibers has been observed in the wavelength range of 1500nm to 1700nm [8]. However, the propagation loss of the guided modes is still to be measured.

In our asymptotic approach, the material absorption is taken into account via the complex dielectric constant. To determine the influence of the material absorption in the cladding layers, we vary the Si absorption from 0dB/cm to 10dB/cm with the remaining parameters held fixed

#2230 - $15.00 US
Received March 14, 2003; Revised April 25, 2003

and calculate the modal loss of the TE01 mode at $1.55\mu m$. The results are shown in Fig. 2(d). The dashed line is a linear fit of the asymptotic results. We find the linear coefficient is $\Gamma = 10^{-4}$, which clearly demonstrates that the cladding material absorption has minimal influence on the guidance of photons in the miniature Bragg fibers.

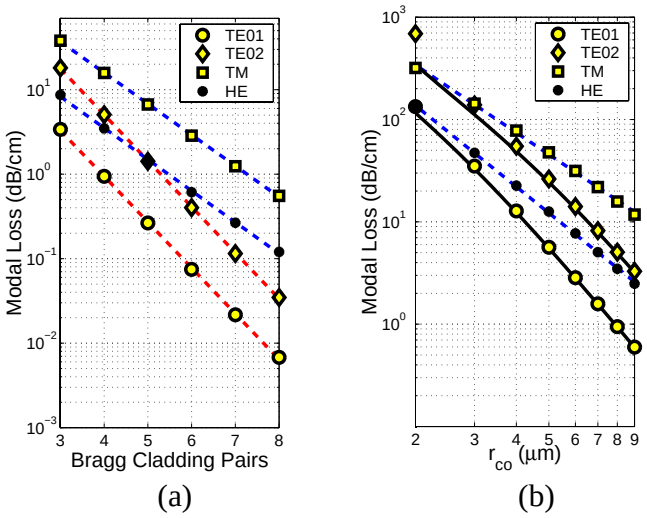

Fig. 3. The loss of the TE01, TE02, TM01, and HE11 modes at $\lambda = 1.55\mu m$. The refractive index and thickness of the cladding layers are the same as in Fig. 2. In (a) we choose the air core radius $r_{co} = 8\mu m$ and vary the Bragg cladding pair number. The dashed lines are the fitting of the asymptotic results using Eq. (9). In (b), we use 4 pairs of Bragg cladding layers and vary the air core radius. The dashed lines are the fitting of the asymptotic results for the TM01 and HE11 modes using Eq. (11). The solid lines are the estimation given by Eq. (12).

3.2 Loss dependence on Bragg cladding pair number and air core radius

To gain more insight into guiding in a Bragg fiber, we investigate the dependence of the modal loss on the number of Bragg cladding pairs and the air core radius. We first fix the air core radius to be $r_{co} = 8\mu m$ and vary the number of Bragg cladding pairs from 3 to 8, with the rest of the fiber parameters held to the same value as those in Fig. 2. Using the asymptotic approach, we calculate the loss of the TE01, TE02, TM01, and HE11 mode at $\lambda = 1.55\mu m$ and show the results in Fig. 3(a). From the asymptotic results, we find that the modal loss dependence on the number of the cladding pairs N is given by:

$$\text{Modal Loss} \propto \Delta^N \,, \tag{9}$$

where Δ is a constant. From fitting the asymptotic results using Eq. (9), we find $\Delta_{TE01} = \Delta_{TE02} = 0.29$, and $\Delta_{TM01} = \Delta_{HE11} = 0.43$. The fitting results are shown in Fig. 3(a) as dashed lines, which are in excellent agreement with the asymptotic results. We notice that the TE modes have similar Δ parameters, whereas the mixed polarization mode and the TM mode share a different Δ parameter. This interesting phenomenon can be understood as a direct result of the decoupling of the TE and the TM components in the Bragg cladding layers. Mathematically speaking, when $m \neq 0$ the presence of the off-diagonal terms such as $(m\beta/k_n^2 r)J_m(k_n r)$ and $(m\beta/k_n^2 r)Y_m(k_n r)$ in Eq. (2) mixes the TE component and the TM component in the "exact solution" region. On the other hand, in the "asymptotic solution" region, the 4×4 transfer matrix becomes block-diagonal, according to Eq. (4). As a consequence, the TE component and the

#2230 - $15.00 US
Received March 14, 2003; Revised April 25, 2003

TM component decay independently in the asymptotic region even for the mixed polarization modes. Since in general the TE component decays much faster than the TM component (see the following discussion), the propagation loss of the mixed polarization modes should share the characteristics of the TM modes.

If the thickness of the cladding layers is close to that of the quarter-wave stack, which is the case for the fiber studied in Fig. 3, the loss decay parameter Δ can also be found using the following simple procedure. According to Ref. [1], a Bragg cladding pair in a quarter-wave stack can reduce the TE mode amplitude by a factor of $\sqrt{\varepsilon_l \omega^2/c^2-\beta^2}/\sqrt{\varepsilon_h \omega^2/c^2-\beta^2}$, where ε_l is the dielectric constant of the low index medium and ε_h is that of the high index medium. For TM modes, the corresponding amplitude reduction factor is $[\varepsilon_l\sqrt{\varepsilon_h \omega^2/c^2-\beta^2}]/[\varepsilon_h\sqrt{\varepsilon_l \omega^2/c^2-\beta^2}]$. Since the modal loss is proportional to the square of the field amplitude outside of the Bragg cladding, we can approximate the loss reduction factor for the TE and non-TE modes as:

$$\Delta_{TE}=\frac{\varepsilon_l-1}{\varepsilon_h-1}\,,\Delta_{non-TE}=\frac{\varepsilon_l^2(\varepsilon_h-1)}{\varepsilon_h^2(\varepsilon_l-1)}\,, \tag{10}$$

where we have substituted the propagation constant β by ω/c. Due to the large core area, this is an excellent approximation, as can also be seen from Fig. 2(b). Using $\varepsilon_l=4.0$ and $\varepsilon_h=12.25$ for the Si/Si_3N_4 cladding, Eq. (10) gives $\Delta_{TE}=0.27$ and $\Delta_{non-TE}=0.40$, quite close to the values of $\Delta_{TE}=0.29$ and $\Delta_{non-TE}=0.43$ obtained from fitting Fig. 3(a) using Eq. (9). The difference might be due to the slight deviation of the Bragg cladding from a quarter-wave stack at $\lambda=1.55\mu m$.

In Fig. 3(b), we choose 4 pairs of Si/Si_3N_4 cladding layers and investigate the variation of the modal loss as we change the air core radius. It was suggested in Ref. [3] that the modal loss for very large core area Bragg fibers (up to $100\mu m$) is inversely proportional to r_{co}^3. However for the miniature Bragg fibers with core area less than $10\mu m$, we find that the $1/r_{co}^3$ relationship no longer holds. In particular, it is clear from the figure that the TE polarized modes and the non-TE polarized obeys different power law dependence. We fit the asymptotic results in Fig. 3(b) assuming

$$\text{Modal Loss}\propto\Big(\frac{1}{r_{co}}\Big)^{\alpha}\,. \tag{11}$$

We find $\alpha_{TE01}=3.61$, $\alpha_{TE02}=3.49$, $\alpha_{TM01}=2.20$, and $\alpha_{HE11}=2.64$.

It has been demonstrated in Ref. [7] that the loss behavior of the TE modes can be modeled by a 1D Bragg stack. In this picture, we can think of the ith TE mode as formed by photons zigzagging within the air core with incident angle $\pi-\theta$, with $\theta=x_{1i}\lambda/2\pi r_{co}$ according to Eq. (8). As shown in Fig. 4, the distance between two consecutive "bounces" should be $2r_{co}/\theta$, assuming a small θ. Denoting the amplitude reflection coefficient of the Bragg cladding is $\mathscr{R}$, we have $\exp(-4\beta_i r_{co}/\theta)=|\mathscr{R}|^2$. For $|\mathscr{R}|^2$ approaching unity, this relation can be rewritten in the dB unit as

$$\text{Modal Loss}=3.46\times10^3\times\frac{x_{1i}\lambda}{r_{co}^2}(1-|\mathscr{R}|^2)\ (\text{dB/cm})\,, \tag{12}$$

where the unit for r_{co} and λ is μm. Comparing Eq. (12) with Eq. (11), we notice that the $1/r_{co}^2$ dependence of the modal loss comes purely from the "geometrical" consideration: The larger the core radius is, the longer the distance between the two consecutive reflections. The rest of the r_{co} dependence of the TE modal loss comes from the reflection coefficient of the 1D Bragg stack. We apply Eq. (12) to estimate the TE modal loss and show the result in Fig. 3(b) as solid lines. It is clear that Eq. (12) provides an excellent approximation for most of the r_{co} values. The only exception is the TE02 modal loss at $r_{co}=2\mu m$, which might be due to a large θ and the reflection coefficient that is no longer close to unity.

#2230 - $15.00 US
Received March 14, 2003; Revised April 25, 2003

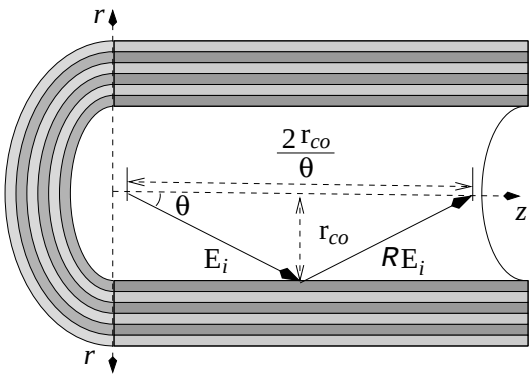

Fig. 4. Estimation of the modal loss from the picture of photons zigzagging within the Bragg fiber.

3.3 Loss dependence on cladding layer thickness

In designing Bragg fibers, it is generally assumed that the quarter-wave stack provides the greatest confinement as cladding layers. For a cladding layer with dielectric constant ε and thickness L, we define a parameter $\Phi = 4\sqrt{\varepsilon - 1}L/\lambda$. For a Bragg fiber with a large air core and consequently $\beta \approx 2\pi/\lambda$, the parameter Φ equals to unity if the cladding layer has exactly quarter wave thickness. For the fiber studied in Fig. 2(c), we find $\Phi_{Si} = 0.98$ for the Si layer and $\Phi_{Si_3N_4} = 0.97$ for the Si_3N_4 layer at $\lambda = 1.5\mu m$. At $\lambda = 1.7\mu m$, the corresponding quantities are, respectively, $\Phi_{Si} = 0.87$ and $\Phi_{Si_3N_4} = 0.86$. Yet at $1.5\mu m$ the Bragg fiber is about four times as lossy as at $1.7\mu m$. This suggests that the quarter-wave stack condition may not lead to lowest propagation loss.

To further investigate this phenomenon, we changed the Si_3N_4 layer thickness from $0.21\mu m$ to $0.19\mu m$, while keeping the rest of the fiber parameters the same as in Fig. 2(c). At $\lambda = 1.5\mu m$, the new Si_3N_4 layer thickness corresponds to $\Phi_{Si_3N_4} = 0.88$. We again calculate the Bragg fiber loss with λ between $1.5\mu m$ and $1.7\mu m$ and plot the results in Fig. 5(b). For the purpose of comparison, we copy Fig. 2(c) as Fig. 5(a). From Fig. 5, it is clear that the reduction of the Si_3N_4 layer thickness leads to both lower loss for the TE01 mode and larger loss penalty for the higher order modes. The solid lines are the loss estimate for the TE modes given by Eq. (12), which again are in excellent agreement with the asymptotic result.

4. Influence of the fiber deformation

In the asymptotic analysis, we assume that the Bragg fibers possess perfect cylindrical symmetry and are uniform along the propagation direction. The experimentally realized Bragg fibers as reported in Ref. [8], however, retain neither of these two properties: The fiber cross-section deviates considerably from the circular shape, and there are gas inlet ports along the fiber propagation direction.

We first use the finite difference time domain (FDTD) algorithm to simulate a Bragg fiber without the cylindrical symmetry but retains uniformity along the propagation direction. Taking advantage of the translational symmetry, we can assume the z dependence of the guided mode as $\exp(-i\beta z)$, where β is the propagation constant. This allows us to take out the z dimension in our FDTD calculations and consider in the simulation only the cross-section of the Bragg fibers. For more details on the FDTD algorithm, the readers can consult Ref. [10].

We limit the FDTD simulations to the TE01 mode and first analyze a Bragg fiber similar to what has been described in the previous section. We set the air core radius to be 300 FDTD cells. The thickness of the Si layer and the Si_3N_4 layer are 6 cells and 12 cells, respectively. By introducing a normalization factor, this FDTD structure represents a Bragg fiber with air core

#2230 - $15.00 US
Received March 14, 2003; Revised April 25, 2003

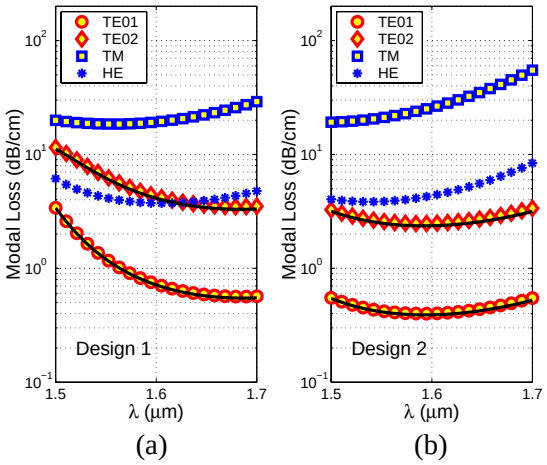

Fig. 5. Asymptotic results for the TE01, TE02, TM01, and HE11 modal loss. The solid lines are the estimation of the TE mode loss given by Eq. (12). In (a), the fiber parameters are the same as used in Fig. 2(c). In (b), we change the Si_3N_4 layer thickness to $0.19\mu m$, while the rest of the parameters remain the same as in (a).

radius of $5.3\mu m$, Si layer thickness $0.11\mu m$, and Si_3N_4 layer thickness $0.21\mu m$. Using FDTD simulations, we calculate the dispersion and the B_z field for both a circularly symmetric Bragg fiber and a deformed Bragg fiber whose upper section is partially flattened. The dispersion of both fibers are plotted in Fig. 6(a), together with a theoretical dispersion curve calculated according to Eq. (8). The theoretical results are in excellent agreement with the FDTD results for the circularly symmetric Bragg fiber, which justify our choice of the simulation parameters. As shown in Fig. 6(a), the dispersion of the deformed fiber is almost the same as that of the cylindrically symmetric fiber, with a small "down-shift" due to the slightly smaller cross-section for the deformed fiber.

The B_z field distribution of the circular Bragg fibers and the deformed Bragg fibers at $\lambda = 1.55\mu m$ are given in Fig. 6(b) and Fig. 6(c). The B_z field in the "flattened" Bragg fiber is essentially that of a TE01 mode. Yet it also has components with non-zero "angular quantum number" m that tend to be much more lossier. In fact, there is clearly some radiation field outside of the deformed Bragg fiber in Fig. 6(c). As a result, a deformed Bragg fiber should have modal loss higher than what is predicted by the asymptotic theory for a cylindrically symmetric fiber, which as shown in Fig. 2(c) is between 0.5-2dB/cm.

The CVD process in the fabrication of the miniature Bragg fiber requires the placement of the gas inlet ports about every 1mm along the fiber propagation direction. The gas inlet port can be regarded as a special case of the Bragg fiber inter-connect as shown in Fig. 7. We can think of channel 1 as the Bragg fiber and channel 2 as the gas inlet port that feeds the gas to be deposited on the surface of the Bragg fiber. In this language, the excessive propagation loss caused by the gas inlet port is the throughput loss of the Bragg fiber inter-connect.

As in Fig. 7, we assume the Bragg fiber has an air core radius of r_1 and the gas inlet port has an air core radius of r_2. One method of calculating the throughput loss is to find the azimuthal component of the electric field at the beginning of the throughput port (denoted by $E_{\theta,t}$ in Fig. (7)). Since the electric field of the TE01 mode has only the azimuthal component $E_{\theta,TE01}$, the throughput loss is simply given by $1-|\int E_{\theta,t}E_{\theta,TE01}\,r\,dr\,d\theta|^2$. The process of finding $E_{\theta,t}$, however, can be very complicated. In the following discussion, we present a much simpler approach by drawing analogy with the free space diffraction of the Gaussian beam. Since the $E_{\theta,t}$ field results from the diffraction of the TE01 mode, we expect the following discussion should at least give us an order of magnitude estimate.

#2230 - $15.00 US
Received March 14, 2003; Revised April 25, 2003

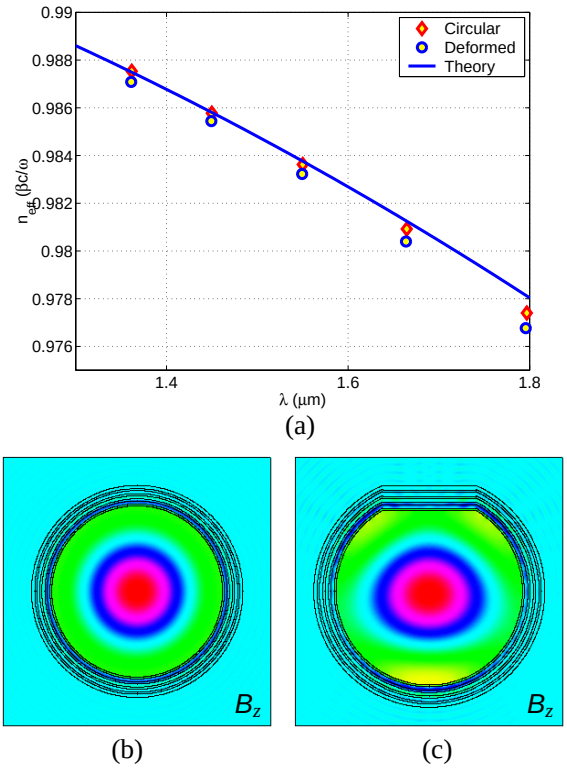

Fig. 6. (a) Dispersion of a Bragg fiber, with air core radius $5.3\mu m$, Si layer thickness $0.11\mu m$ and Si_3N_4 layer thickness $0.21\mu m$. The diamonds and the circles respectively represent the dispersion of the cylindrically symmetric fibers and the deformed fibers, calculated from FDTD simulations. The solid line is given by Eq. (8). In (b) and (c), we show the B_z field of the TE01 mode at $\lambda = 1.55\mu m$ in the circularly symmetric Bragg fiber and the deformed Bragg fiber.

For a Gaussian beam with minimal spot size w_0, the evolution of the beam spot size $w(z)$ follows [11]:

$$[w(z)]^2 = w_0^2(1+\frac{z^2}{z_0^2}) \ , \ z_0 = \frac{\pi w_0^2}{\lambda} \ . \tag{13}$$

In order to approximate the diffraction of the TE01 mode by a Gaussian beam, we need to find its equivalent minimal spot size w_0. According to Eq. (8), the far field divergence angle θ of the TE01 mode is $\theta = x_{11}\lambda/(2\pi r_1)$, whereas the far field divergence angle of a Gaussian beam is given by $\theta = \lambda/\pi w_0$ [11]. Equalizing the two divergence angles, we find $w_0/r_1 = 2/x_{11} \approx 0.52$, which has the right order of magnitude since the minimal spot size w_0 should be less than the Bragg fiber radius r_1. Substituting this result into Eq. (13), we find

$$\left[\frac{w_0}{w(z)}\right]^2 = \frac{1}{1+\frac{z^2\lambda^2 x_{11}^4}{16\pi^2 r_1^4}} \ . \tag{14}$$

Since $w(z)^2$ is proportional to the cross-section area of the Gaussian beam, the amount of light that is coupled back into the throughput port can be approximated by $[w_0/w(z)]^2$. Set $z = 2r_2$ and use dB unit, we find:

$$\text{Throughput Loss} = 23.7\frac{r_2^2\lambda^2}{r_1^4} \ (\text{dB}). \tag{15}$$

#2230 - $15.00 US
Received March 14, 2003; Revised April 25, 2003

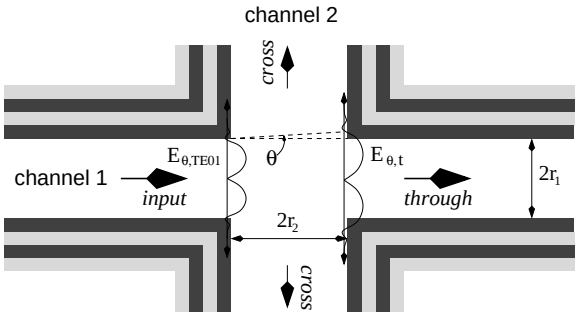

Fig. 7. Schematics of a Bragg fiber inter-connect.

Use the value of $r_1 = 7.5\mu m$, $r_2 = r_1/2$, and $\lambda = 1.55\mu m$, we find the throughput loss is 0.25dB. We notice that the the loss has a $1/r_1^4$ dependence. If we keep the rest of the parameters and increase air core radius by 50%, the throughput loss is decreased by a factor 5.

5. Conclusion

In conclusion, we extend the asymptotic model developed in Ref. [4] and [5] to include the Bragg fiber propagation loss due to the finite cladding layer thickness and the material absorption. We analyze air-core Bragg fibers with Si/Si_3N_4 cladding pairs, which were fabricated using chemical vapor deposition (CVD) [8], and demonstrate that it is possible to achieve propagation loss below 1dB/cm with only 4 pairs of Si/Si_3N_4 cladding layers. We find that the material absorption in the cladding layers has little impact on the fiber propagation loss. We also give a simple formula that describes the reduction of fiber propagation loss as we increase the number of cladding pairs. We use a finite-difference time-domain (FDTD) algorithm to investigate the impact of fiber deformation on the modal propagation characteristics. Finally, a simple Gaussian beam approximation is applied to evaluate the additional loss due to the existence of the gas inlet ports introduced in the CVD fabrication processes.

This research was sponsored by the Office of Naval Research (Y. S. Park), whose support is gratefully acknowledged.

#2230 - $15.00 US
Received March 14, 2003; Revised April 25, 2003